Benchmark of TJ Code Against STRIDE Code

R. Fitzpatrick [a]

Institute for Fusion Studies, Department of Physics,

University of Texas at Austin, Austin TX 78712, USA

I. SYMMETRY RELATIONS

Let all lengths be normalized to the major radius of the magnetic axis, R_0, and let all magnetic field-strengths be normalized to the toroidal magnetic field-strength at the axis, B_0. Consider an axisymmetric toroidal plasma equilibrium. Let R, ϕ, Z be a conventional cylindrical coordinate system that is co-axial with the toroidal symmetry axis of the plasma. The equilibrium magnetic field is written

$$\mathbf{B} = \nabla\phi \times \nabla\psi + g(\psi)\,\nabla\psi, \tag{1}$$

where ψ is the poloidal magnetic flux. We can also define

$$\Psi_N = \frac{\psi}{\psi_a}, \tag{2}$$

where ψ_a is the poloidal flux at the plasma boundary. Thus, $\Psi_N = 0$ at the magnetic axis, and $\Psi_N = 1$ on the plasma boundary. In the following, it is assumed that Ψ_N is the 'radial' coordinate in STRIDE.

Let

$$L^m_m(\Psi_N) = I(\Psi_N)\left(J(\Psi_N)\left[\frac{m\,g(\Psi_N)}{q(\Psi_N)}\right]^2 + [n\,\psi_a]^2\right), \tag{3}$$

$$I(\Psi_N) = \int_0^{\Psi_N} \frac{2\,q\,(\Psi'_N)}{g(\Psi'_N)}\,d\Psi'_N, \tag{4}$$

$$J(\Psi_N) = \oint |\nabla\Psi_N|^{-2}\,\frac{d\theta}{2\pi}, \tag{5}$$

$$\rho(\Psi_N) = \frac{I(\Psi_N)\,g(\Psi_N)}{q(\Psi_N)}, \tag{6}$$

$$s(\Psi_N) = \frac{d\ln q}{d\Psi_N}, \tag{7}$$

[a] rfitzp@utexas.edu

where m is a poloidal mode number, n is a toroidal mode number, $q(\Psi_N)$ is the safety-factor, and θ is a 'straight' poloidal angle defined such that

$$(\nabla\phi \times \nabla\theta \cdot \nabla\phi)^{-1} = \frac{q\,R^2}{g}, \tag{8}$$

Note that we are working in PEST coordinates.

Let m_j be the poloidal mode number of the jth rational surface, which is located at $\Psi_N = \Psi_{N\,j}$. Let $D_{I\,j}$ be the ideal Mercier index at the jth rational surface, and let

$$\nu_{L\,j} = \frac{1}{2} - \sqrt{-D_{I\,j}}, \tag{9}$$

$$\nu_{S\,j} = \frac{1}{2} + \sqrt{-D_{I\,j}}. \tag{10}$$

Let

$$f_{L\,j} = \left[\rho^{\nu_{L\,j}} \left(\frac{\nu_{S\,j} - \nu_{L\,j}}{L_{m_j}^{m_j}}\right)^{1/2} s\,m_j\right]_{\Psi_{N\,j}}, \tag{11}$$

$$f_{S\,j} = \left[\rho^{\nu_{S\,j}} \left(\frac{\nu_{S\,j} - \nu_{L\,j}}{L_{m_j}^{m_j}}\right)^{1/2} s\,m_j\right]_{\Psi_{N\,j}}. \tag{12}$$

Finally, let

$$\hat{A}_{ij} = f_{S\,j}\,A_{ij}\,f_{L\,j'}^{-1}, \tag{13}$$

$$\hat{B}_{ij} = f_{S\,j}, B_{ij}\,f_{L\,j'}^{-1}, \tag{14}$$

$$\hat{\Gamma}_{ij} = f_{S\,j}\,\Gamma_{ij}\,f_{L\,j'}^{-1}, \tag{15}$$

$$\hat{\Delta}_{ij} = f_{S\,j}, \Delta_{ij}\,f_{L\,j'}^{-1}, \tag{16}$$

where A_{ij}, B_{ij}, Γ_{ij}, and Δ_{ij} are the elements of the outer matching matrices calculated by STRIDE, whereas the hatted quantities are the corresponding matching matrices calculated by TJ. Equations (77) and (100) of Ref. 1 imply that

$$\hat{A}_{ji}^* = \hat{A}_{ij}, \tag{17}$$

$$\hat{\Delta}_{ji}^* = \hat{\Delta}_{ij}, \tag{18}$$

$$\hat{B}_{ji}^* = \hat{\Gamma}_{ij}. \tag{19}$$

These symmetries are ultimately due to the self-adjoint nature of the ideal-MHD force operator. However, as explained in Ref. 2, the symmetries can also be related to the conservation

of toroidal electromagnetic angular momentum. The symmetries have to be respected by a toroidal tearing mode code, otherwise the code would predict that an isolated plasma could exert a net toroidal electromagnetic torque on itself. Note that, in the cylindrical limit, $\hat{\Delta}_{jj}$ is equivalent to $r_s\,\Delta'$: i.e., the tearing stability index normalized to the minor radius of the rational surface.

II. TJ/STRIDE LARGE ASPECT-RATIO CIRCULAR EQUILIBRIUM

The TJ/STRIDE large-aspect ratio, circular, plasma equilibrium has a Wesson-like current profile [3] characterized by the safety-factor on the magnetic axis, q_0, and the safety-factor at the plasma boundary, q_a. The equilibrium is also characterized by the inverse aspect-ratio of the plasma, ϵ_a.

In TJ, the lowest-order safety-factor profile is written

$$q(r) = \frac{q_c\,\nu\,(r/a)^2}{1-[1-(r/a)^2]^\nu}, \tag{20}$$

and the pressure profile takes the form

$$p(r) = p_c\,\epsilon_a^2\left[1-\left(\frac{r}{a}\right)^2\right]^\mu. \tag{21}$$

Here, r is the flux surface label with dimensions of length defined in Ref. 4. Moreover, the magnetic axis corresponds to $r=0$, and the plasma boundary to $r=a$. The value of ν is adjusted to obtain the desired value of $q_a = q(a)$.

The STRIDE parallel current profile, $\sigma = \mathbf{J}\cdot\mathbf{B}/B^2$, is written

$$\sigma(r) = \frac{2}{q_0}\left[1-\left(\frac{r}{a}\right)^2\right]^{p_\sigma}. \tag{22}$$

whereas the pressure profile takes the form

$$p(r) = \frac{\beta_0}{2}\left[1-\left(\frac{r}{a}\right)^2\right]^{p_p}. \tag{23}$$

A STRIDE equilibrium is defined by the parameters q_0, p_σ, β_0, and p_p. In TJ equilibria, $q_c = q_0$, $\mu = p_p$, and $p_c = \beta_0/(2\,\epsilon_a^2)$, but ν is adjusted to obtain the same q_a value as in STRIDE. TEAR equilibria are specified by $\epsilon_a = 0$, q_0, and q_a.

III. BENCHMARK TESTS

A. Single Rational Surface

We consider the stability of $n = 1$ tearing modes in a zero pressure equilibrium that only contain a single $n = 1$ rational surface: namely, the 2/1 surface.

1. Test 1

The first test has equilibria characterized by $q_0 = 1.1$ and $p_\sigma = 1.36$, with a range of different inverse aspect-ratios, ϵ_a. Figure 1 compares the $\hat{\Delta}_{11}$ (i.e., the tearing stability index of the 2/1 tearing mode) values calculated by the TJ code,[4] the TEAR code (which is a cylindrical tearing mode code), and the STRIDE code. It can be seen that the tearing stability indices calculated by the TJ and STRIDE are in good agreement, and asymptote to that calculated by the TEAR code in the cylindrical limit, $\epsilon_a \rightarrow 0$.

2. Test 2

The second test has equilibria characterized by $q_0 = 1.1$ and $\epsilon_a = 0.2$, with a range of edge safety-factor values, q_a. Figure 2 compares the $\hat{\Delta}_{11}$ (i.e., the tearing stability index of the 2/1 tearing mode) values calculated by the TJ code, the TEAR code, and the STRIDE code. It can be seen that the tearing stability indices calculated by the TJ and STRIDE are in good agreement, except when the $q = 3$ surface closely approaches the plasma boundary (i.e., $q_a \rightarrow 3$).

B. Two Rational Surfaces

We consider the stability of $n = 1$ tearing modes in an equilibrium that contains two $n = 1$ rational surface: namely, the 2/1 surface and the 3/1 surface.

1. Test 3

The third test has equilibria characterized by $q_0 = 1.1$ and $\epsilon_a = 0.2$, with a range of edge safety-factor values, q_a. Figure 3 compares the elements of the tearing stability matrix, $\hat{\Delta}_{ij}$, calculated by the TJ and the STRIDE codes. It can be seen that the elements calculated by TJ and STRIDE are in good agreement. In particular, both codes predict that $\mathrm{Im}(\hat{\Delta}_{11}) = \mathrm{Im}(\hat{\Delta}_{22}) \simeq 0$ and $\hat{\Delta}_{21} \simeq \hat{\Delta}_{12}^*$, as should be the case, according to Eq. (18).

2. Test 4

The fourth test has equilibria characterized by $q_0 = 1.1$, $\epsilon_a = 0.2$, $p_\sigma = 2.1$, and $p_p = 2.0$, with a range of β_0 values. Figure 4 compares the elements of the tearing stability matrix calculated by the TJ and the STRIDE codes. The TJ β_0 values have been rescaled by a factor 1.08 to compensate for the slightly different β-limits in the slightly different TJ and STRIDE equilibria. Once this correction has been made, it can be seen that the elements calculated by TJ and STRIDE are in reasonably good agreement. Again, both codes predict that $\mathrm{Im}(\hat{\Delta}_{11}) = \mathrm{Im}(\hat{\Delta}_{22}) \simeq 0$ and $\hat{\Delta}_{21} \simeq \hat{\Delta}_{12}^*$, as should be the case, according to Eq. (18).

REFERENCES

[1] A. Pletzer, A. Bondeson, and R.L. Dewar, J. Comp. Phys. **115**, 530 (1994).

[2] R. Fitzpatrick, Phys. Plasmas **1**, 3308 (1994).

[3] J.A. Wesson, Nucl. Fusion **18**, 87 (1978).

[4] R. Fitzpatrick, Phys. Plasmas **31**, 102507 (2024).

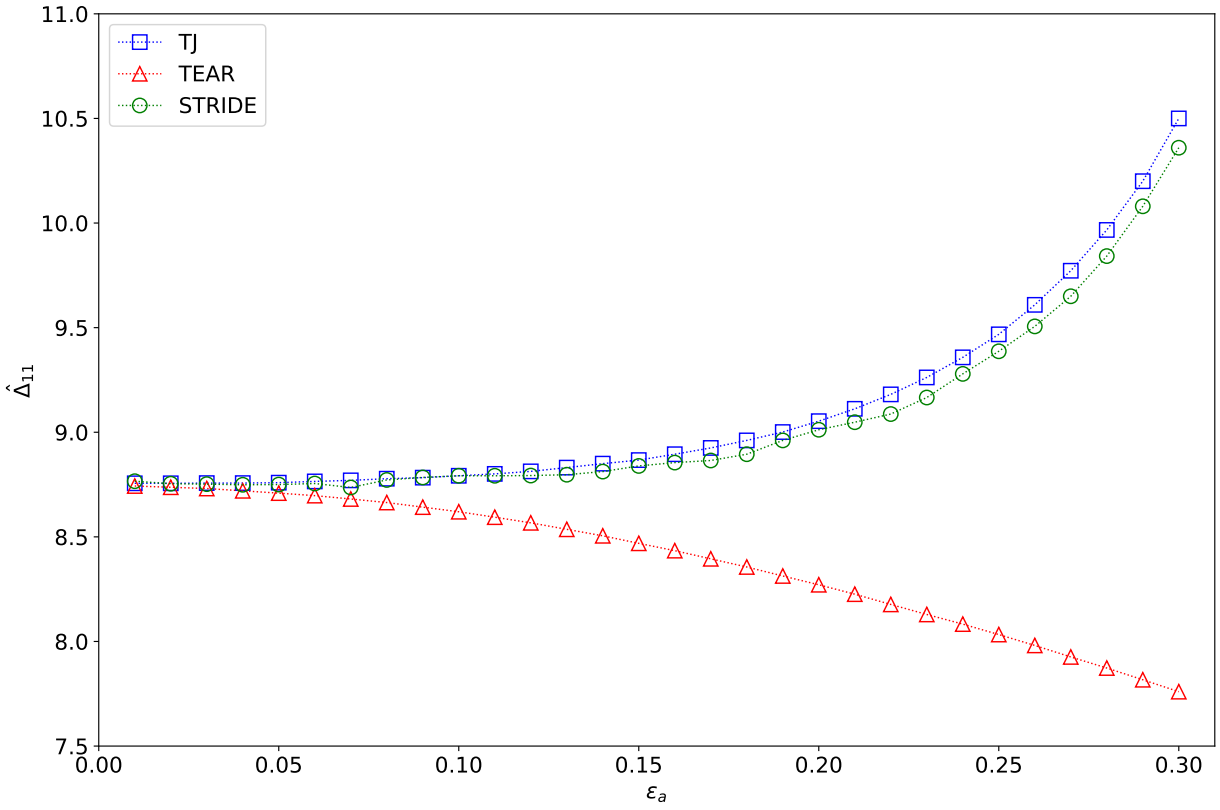

FIG. 1. Test 1: $q_0 = 1.1$, $p_\sigma = 1.36$, $\beta_0 = 0.0$. Variation of 2/1 tearing stability index with inverse-aspect ratio, ϵ_a.

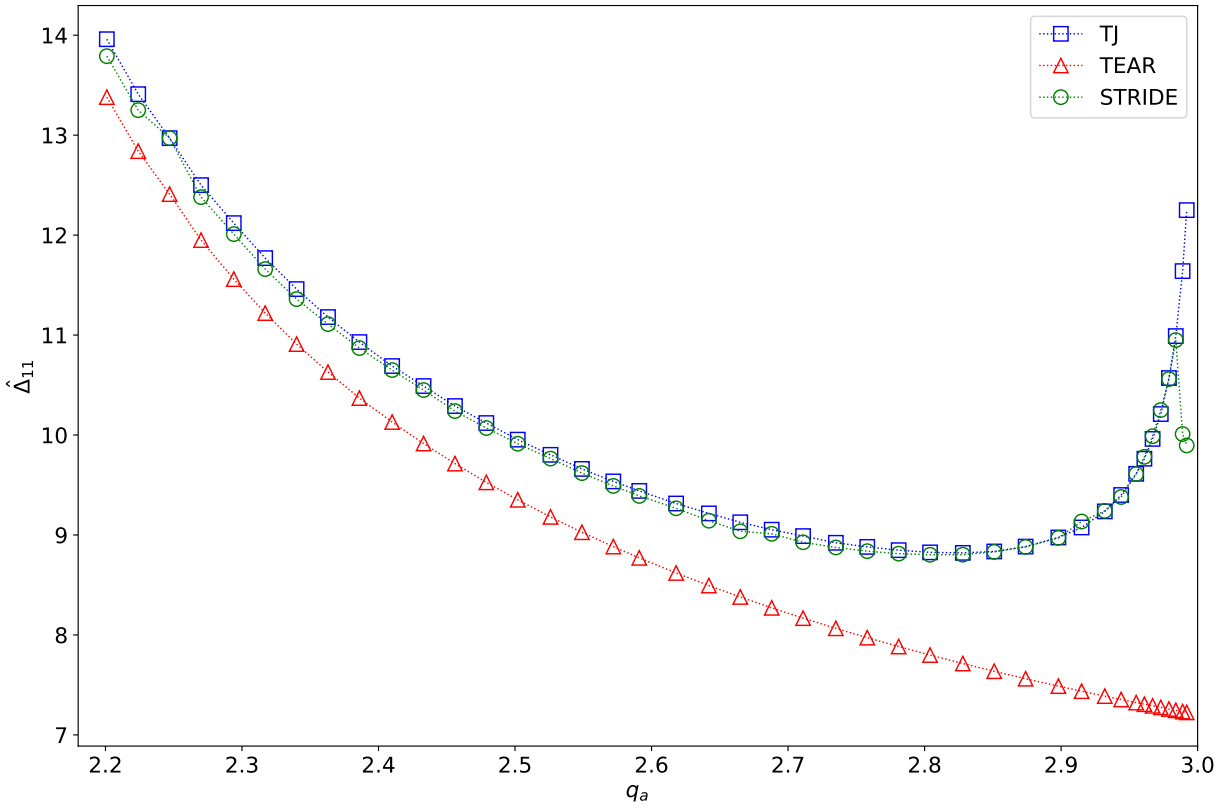

FIG. 2. Test 2: $q_0 = 1.1$, $\epsilon_a = 0.2$, $\beta_0 = 0.0$. Variation of 2/1 tearing stability index with q_a.

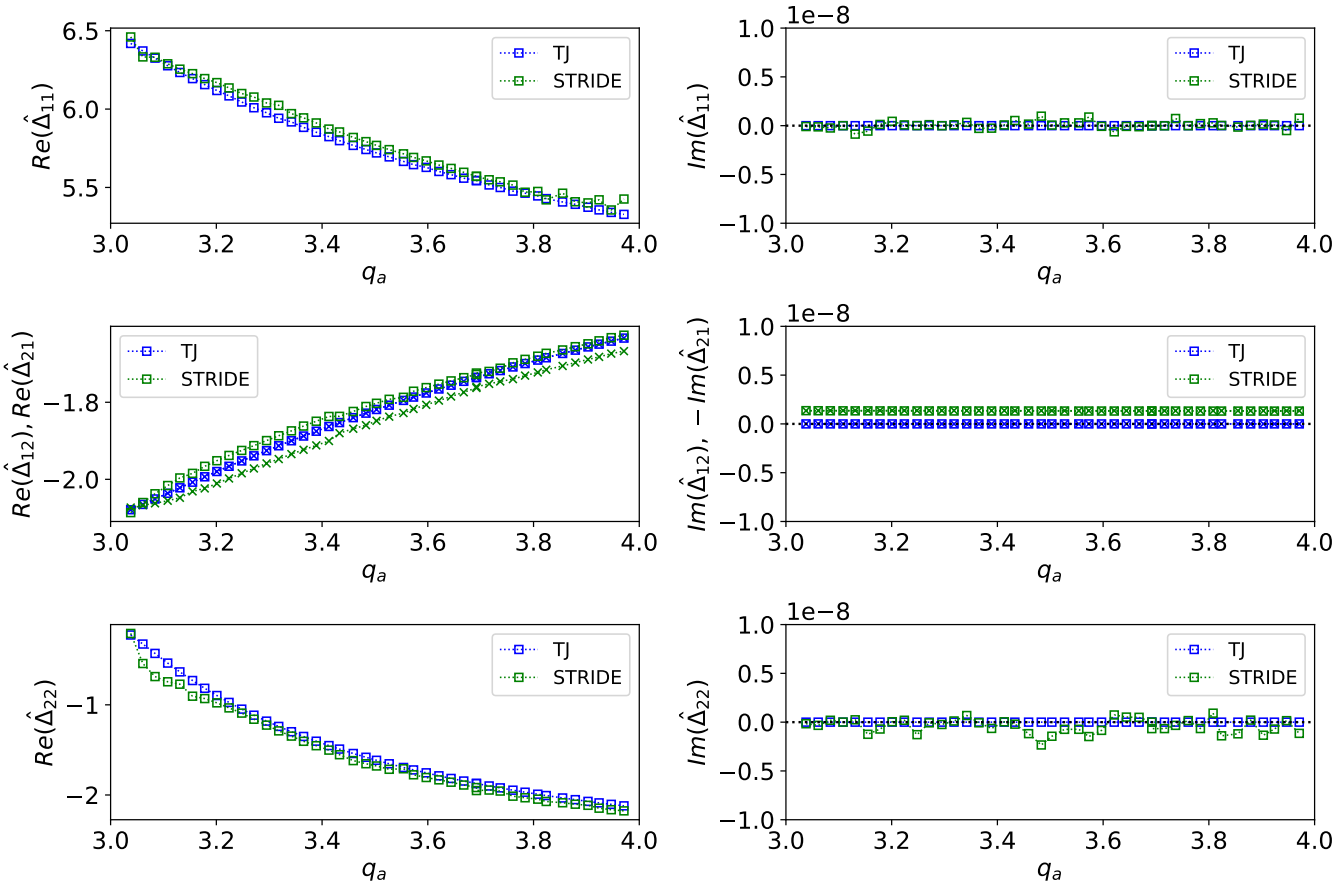

FIG. 3. Test 3: $q_0 = 1.1$, $\epsilon_a = 0.2$, $\beta_0 = 0.0$. Variation of elements of tearing stability matrix with q_a. In the middle panels the squares indicate $\hat{\Delta}_{12}$ and the crosses indicate $\hat{\Delta}_{21}$.

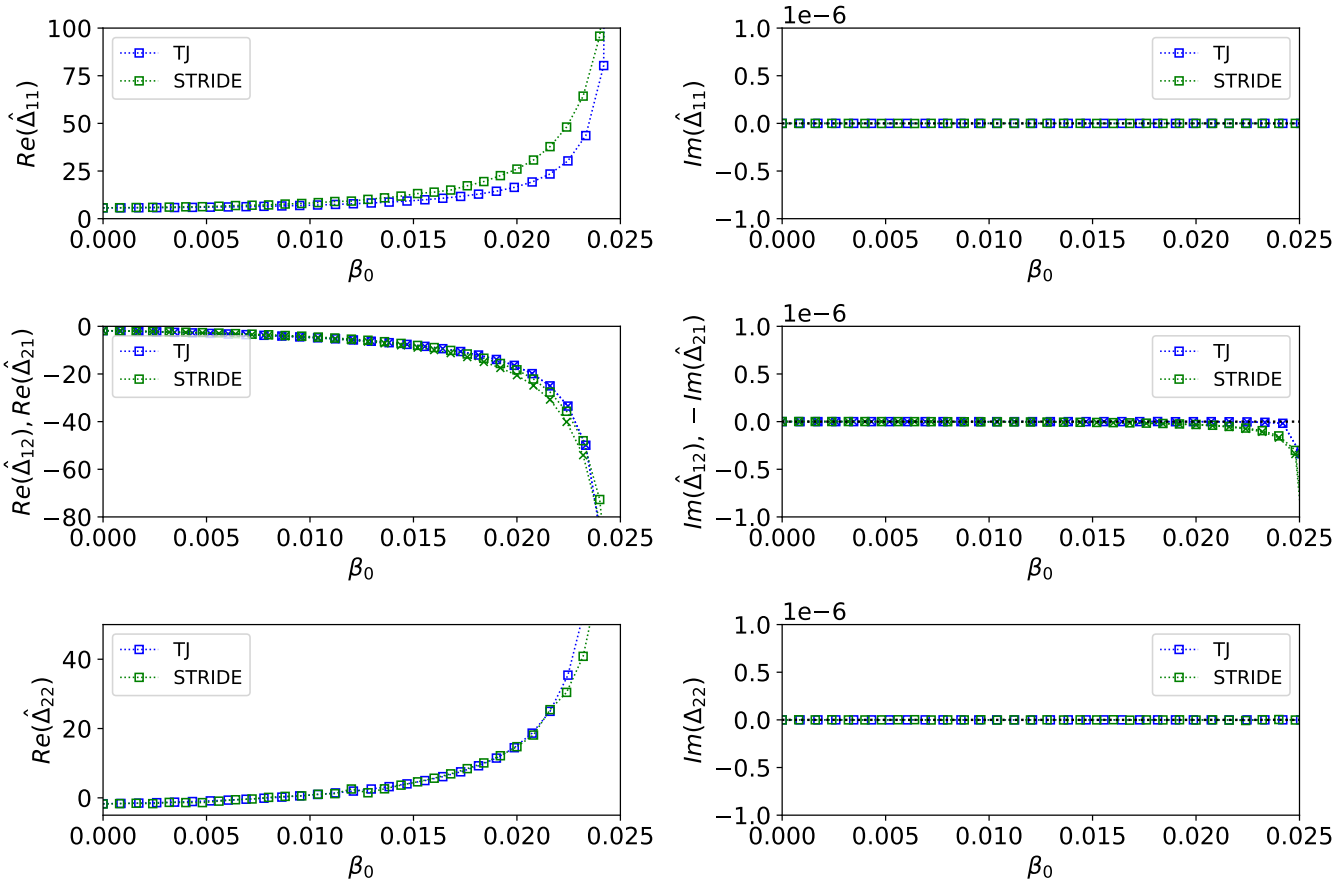

FIG. 4. Test 3: $q_0 = 1.1$, $\epsilon_a = 0.2$, $p_\sigma = 2.1$, and $p_p = 2.0$. Variation of elements of tearing stability matrix with β_0. In the middle panels the squares indicate $\hat{\Delta}_{12}$ and the crosses indicate $\hat{\Delta}_{21}$. The TJ β_0 has been rescaled by a factor 1.08.